Available online at www.sciencedirect.com

Chemical Engineering Research and Design

journal homepage: www.elsevier.com/locate/cherd

New robust approach for the globally optimal design of fired heaters

Sung Young Kim[a], Andre L.H. Costa[b], Miguel J. Bagajewicz[b,c,d,*]

[a] Department of Chemical Engineering, Dong-A University, Busan, South Korea
[b] Institute of Chemistry, Rio de Janeiro State University (UERJ), Rio de Janeiro, Brazil
[c] Escola de Química CT, Federal University of Rio de Janeiro (UFRJ), Rio de Janeiro, RJ, Brazil
[d] Department of Chemical, Biological & Materials Engineering, University of Oklahoma, Norman, OK, United States

ARTICLE INFO

Article history:
Received 21 February 2023
Received in revised form 1 July 2023
Accepted 1 August 2023
Available online 3 August 2023

Keywords:
Fired Heaters
Optimization
Global Optimum

ABSTRACT

Fired heaters are important components of heat exchanger network (HEN) synthesis, especially in view of the existing procedures to simultaneously synthesize the HEN and obtain the basic design of heat exchangers. Existing basic design procedures for fired-heaters are either too simple, or difficult to solve when based on MINLP procedures. In addition, CFD approaches can hardly be used in design optimization and metaheuristics do not guarantee global optimality. We present two novel advances: a reformulation of models from previous optimization literature and we use Partial and Proxy Set Trimming followed by Smart Enumeration, a recently introduced robust technique. The proposed approach does neither needs initial solutions, nor does it have convergence problems and it also guarantees global optimality. The Set Trimming variant, namely Proxy Set Trimming, which was not part of the original Set Trimming version of Set Trimming is also used.

1. Introduction

Most of the energy consumption in oil refining, and petrochemical industries attending high-temperature heating occurs fired heaters. Efficiency improvement through the optimal design of fired heaters decreases energy consumption and cost.

Aside from the need for a robust stand-alone basic design of fired heaters, an automatic design model that can guarantee global optimality is also needed for the simultaneous synthesis of heat exchanger network (HEN) and the basic design of heat exchangers (Ponce-Ortega et al.,2007; Xiao et al., 2019; Silva et al., 2008; Mizutani et al.,2003; Ravagnani and Caballero, 2007; Jin et al., 2008; Short et al. (2016); Kazi et al., 2021). All the aforementioned approaches do not include the design of fired heaters or steam-based heaters. We intend to fill this gap with our model and solution procedure.

A fired heater consists of three main sections: radiant and convection sections, and a stack. Heat transfer only occurs in the radiant and convection section, whereas the stack is responsible to exhaust the flue gas to the atmosphere and also provides the draft in fired heaters not associated with mechanical draft.

Wimpress (1978) discussed the computing of the performance of the radiation and the convection section of the direct-fired heaters and determined the set of equations needed for it. Ibrahim and Al-Qassimi (2010) used a simplified model to simulate the heat transfer in the convection section in process fired heaters. Later they studied the flame

* Corresponding author at: Institute of Chemistry, Rio de Janeiro State University (UERJ), Rio de Janeiro, Brazil.
E-mail address: bagajewicz@ou.edu (M.J. Bagajewicz).
https://doi.org/10.1016/j.cherd.2023.08.002
0263-8762/

and firebox temperature effects on heat transfer (Ibrahim, Al-Qassim, 2013). They used the procedure presented by Couper et al. (2012) for the cabin-type fired heater. In these two studies, there is no attempt to use the model to perform a design. Masoumi and Izakmehri (2011) developed a simplified mathematical model to be used for simulation. They also claim that they developed a design optimization procedure. This design optimization method is only based on studying the variations of excess air, air temperature, and the addition of area to an existing furnace. Also, using simulations for a given fired heater, they quantified the effect of excess air and air temperature on its efficiency. Varghese and Bandyopadhyay (2012) proposed the methodology for the area-energy targeting of a single-zoned fired heater in a heat exchanger network. The targeting is based on the logarithmic mean temperature difference (LMTD) method for the convection section.

Mussati et al. (2009) published the first mathematical programming-based article on the design of a fired heater using a mixed-integer nonlinear model. They minimized two objectives: area and total annualized cost. The model cannot be solved using mixed-integer nonlinear programming without initial values and even when initial values are provided, its optimum is local, not guaranteed to be global. In addition, the model used relies on certain heuristics-based correlations that are not based on first principles. Later, Jethva and Bhagchandani (2013) proposed a model and implemented it in Microsoft Excel. The article claims that it designs the heater, but it is unclear what procedure is used. We assume that Excel's "solver" has been used so initial values must have been used and a local solution is expected at best. A particular solution, presumably obtained in a design mode, was obtained using the HTRI heat exchanger suite 6.0. While the authors claim the results are satisfactory, the results differ significantly. Karimi et al. (2019), also presented a model in Microsoft Excel solving similar equations and focusing on steam generation.

Jegla et al. (2016) discuss the proper design of combustion and radiant chambers with inbuilt heat transfer surfaces, a valuable contribution, but no optimization mathematical model is presented. Haratian et al. (2019) developed a detailed model and optimized the design using a Genetic Algorithm (GA). The number of geometric variables considered is limited and the model is simplified. The results are not guaranteed optimal, much less globally optimal.

This paper addresses the optimal basic design of fired heaters. The goal is to identify the design alternative that can fulfill the desired thermal duty, associated with the lowest total annualized cost (TAC). Our approach to solving this problem consists of Set Trimming followed by Smart Enumeration (Costa and Bagajewicz, 2019). We start with listing all discrete geometric variables that are independent, that is, we pick the minimum set of variables that, once fixed, renders a complete heater geometry and allows the calculation of its performance. Such a design may or may not be viable because it violates some inequality constraints. Thus, the list of solution candidates is first screened to eliminate those alternatives that are infeasible under inequality constraints. For this, we use constraints that are explicit in the model and also proxy constraints, which consist of model constraints or a subset of constraints that are evaluated using limiting values, or new constraints that have the same conceptual origin as the existing ones (mostly energy balances). After Set Trimming, Smart Enumeration follows. Smart Enumeration consists of ordering all candidates by their lower bound of the objective function first. Next, the candidates are evaluated rigorously one by one, keeping the incumbent best solution, and stopping when the value of the lower bound is larger than the incumbent.

The article is organized as follows: We first present the model. Next, we illustrate the particulars of the Set Trimming and Smart Enumeration procedures as they apply to this problem. We finish presenting results and a discussion.

2. Fired heater model

We base our design on the general structure shown in Fig. 1. We reproduce here the most relevant equations used to model the fired heater. Most of them are similar to those used by Mussatti et al. (2009), but with many additions and modifications to adjust the model better to practical geometries and to replace some heuristics-based equations with ones based on first principles. We assume that oil is the process stream that is heated, but the model can be adapted to the use of any other stream type (gaseous or two-phase streams).

We point out that, in our case, in the convection section, the tubes are finned, except the shield tubes. Additionally, without loss of generality, we assume there is only one row of shield tubes. The independent geometric variables are:

1. Length of the radiation and convection sections (L),
2. Number of passes (N_{passes}),
3. Number of tubes per pass per row in the convection section (Nt_{conv}^{pass}),
4. Number of rows of finned tubes in the convection section (Nr_{conv}) (these do not include the row of shield tubes; although the shield tubes belong to the convection section, thus affecting the calculation of the height of the convection section, from the point of view of heat transfer they are bare tubes subject to radiation).
5. Number of tubes per pass in the ceiling and side walls of the radiation section (Nt_{rad}^{pass}),
6. Number of tubes in the ceiling (Nt_{rad}^{ceil}),
7. Height of the stack above the convection section (H_s),
8. Diameter of the stack (D_s) and its thickness (t_s), without loss of generality, we assume that these options are available in pairs (D_s, t_s),
9. Outer tube diameters of the convection and radiation sections (d_o^{rad} and d_o^{conv}) and its associated wall thickness (t_d^{rad} and t_d^{conv}), available in pairs (d_o^{rad}, t_d^{rad})and (d_o^{conv}, t_d^{conv}); the choices are made using standard options),
10. Tube pitch ratio of the radiation section (r_p^{rad}) (i.e. the ratio between the distance of the centers of adjacent tubes and the outlet tube diameter). (Fig. 2),
11. Transverse tube pitch ratio (horizontal direction) of the convection section ($r_p^{conv,h}$) (i.e. the ratio between the distance of the centers of adjacent tubes of the same row and the outlet tube diameter) (Fig. 2),

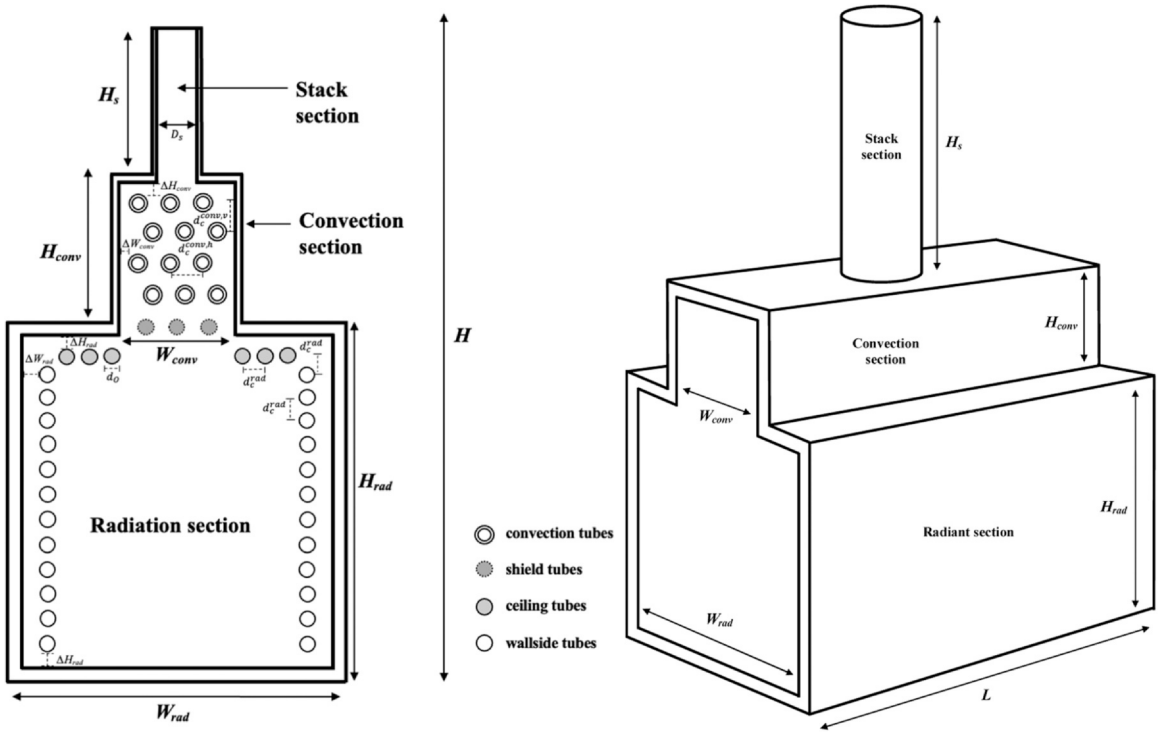

Fig. 1 – Fired heater geometry.

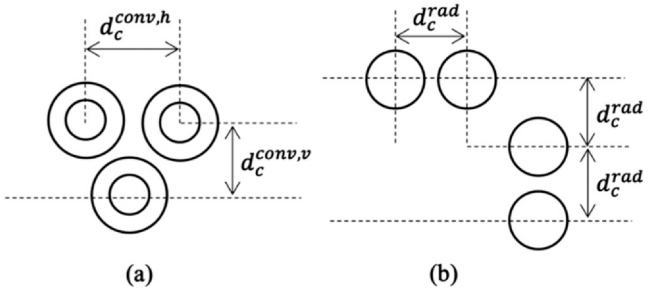

Fig. 2 – Front view of (a) finned tubes and (b) ceiling tubes and wall side tubes.

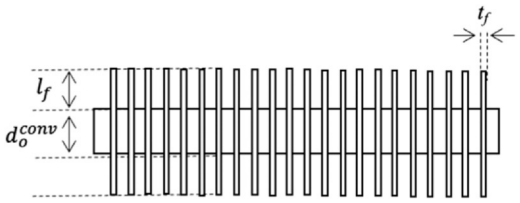

Fig. 3 – Side view of a finned tube.

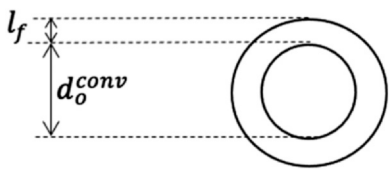

Fig. 4 – Front view of a finned tube.

12. Longitudinal pitch ratio (vertical direction) of the convection section ($r_p^{conv,v}$) (i.e. the ratio between the distance of the center planes of adjacent tube rows and the outlet tube diameter) (Fig. 2),
13. Finned surface alternatives of the convection section, that is, the set of values of fin thickness (t_f), fin height (l_f), and the number of fins per unit length (N_f) in the convection section (see Figs. 3, 4, and 5), these alternatives are available in triplets (t_f, l_f, N_f), associated with a given pair of outer tube diameter and thickness (d_o^{conv}, t_d^{conv}), as usually presented by the manufacturers.

The values that are known beforehand or correlation parameters are shown in the model below with the symbol "^" on top.

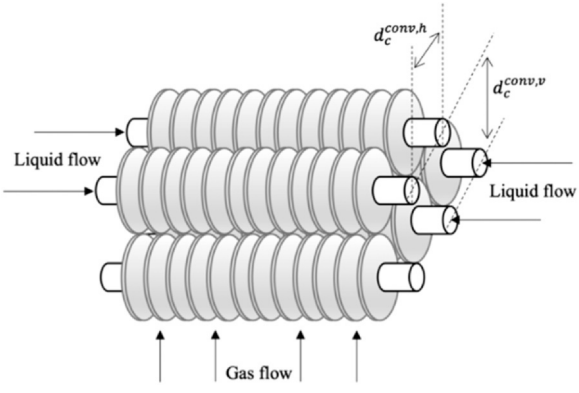

Fig. 5 – Perspective view of the finned tube bundle.

The dependent geometric variables are: the internal diameter of each tube (d_i^{rad} and d_i^{conv}), the diameter of the fin (d_f), the number of tubes in the convection section (Nt_{conv}), the number of tubes in the assumed single row of shield tubes (Nt_{shield}) (the number of tubes in each row of the convection section as well as in the shield tubes row is equal), the number of tubes on the side walls ($Nt_{rad}^{sidewall}$), the total number of tubes in the radiation section (Nt_{rad}) (also including the shield tubes), the distance between the centers of adjacent tubes in the radiation section (d_c^{rad}), the height and width of the radiation section (H_{rad} and W_{rad}), the distance between the centers of adjacent tubes of the same row ($d_c^{conv,h}$), the distance between the center planes of adjacent tube rows ($d_c^{conv,v}$), the height and width of the convection section (H_{conv} and W_{conv}), and the exposed length of the tubes (E_l).

The dependent variables are obtained as follows:

$$d_i^{rad} = d_o^{rad} - 2t_d^{rad} \tag{1}$$

$$d_i^{conv} = d_o^{conv} - 2t_d^{conv} \tag{2}$$

$$d_f^{conv} = d_o^{conv} + 2l_f \tag{3}$$

$$Nt_{conv} = Nt_{conv}^{pass} N_{passes} Nr_{conv} \tag{4}$$

$$Nt_{shield} = Nt_{conv}^{pass} N_{passes} \tag{5}$$

$$Nt_{rad}^{sidewall} = Nt_{rad}^{pass} N_{passes} - Nt_{rad}^{ceil} \tag{6}$$

$$Nt_{rad} = Nt_{rad}^{pass} N_{passes} + Nt_{shield} \tag{7}$$

$$d_c^{rad} = d_o^{rad} r_p^{rad} \tag{8}$$

$$H_{rad} = \left(\frac{Nt_{rad}^{sidewall}}{2}\right) d_c^{rad} + d_o + 2\,\Delta H_{rad} \tag{9}$$

$$W_{rad} = 2\left[\left(\frac{Nt_{rad}^{ceil}}{2}\right) d_c^{rad} + d_o^{rad} + \Delta W_{rad}\right] + W_{conv} \tag{10}$$

$$d_c^{conv,h} = d_o^{conv} r_p^{conv,h} \tag{11}$$

$$d_c^{conv,v} = d_o^{conv} r_p^{conv,v} \tag{12}$$

$$H_{conv} = (Nr_{conv} + 1) d_c^{conv,v} + \frac{d_o^{conv}}{2} + \frac{d_f}{2} + \Delta H_{conv} \tag{13}$$

$$W_{conv} = (Nt_{conv}^{pass} \quad N_{passes} - 1) d_c^{conv,h} + \frac{d_c^{conv,h}}{2} + d_f + 2\,\Delta W_{conv} \tag{14}$$

$$E_l = L - \hat{k}_l \tag{15}$$

where $\hat{k}_l$ is the unexposed portion of the tubes (a parameter independent of the tube length used), ΔH_{rad} and ΔW_{rad} are the clearances between the tubes and the ceiling and the side wall respectively, which are given by:

$$\Delta H_{rad} = \hat{\delta}_{H_{rad},1} + \hat{\delta}_{H_{rad},2}\, d_o^{rad} \tag{16}$$

$$\Delta W_{rad} = \hat{\delta}_{W_{rad},1} + \hat{\delta}_{W_{rad},2}\, d_o^{rad} \tag{17}$$

and ΔH_{conv} is the clearance between the fin tip of the upper row of tubes in the convection section and the end of the convection section and ΔW_{conv} is the clearance between the fin tip of the tubes in the convection section and the convection section walls, which can be estimated by:

$$\Delta H_{conv} = \hat{\delta}_{H_{conv},1} + \hat{\delta}_{H_{conv},2}\, d_f \tag{18}$$

$$\Delta W_{conv} = \hat{\delta}_{W_{conv},1} + \hat{\delta}_{W_{conv},2}\, d_f \tag{19}$$

Shield tubes belong to the convection section, but because they are exposed to radiation from the combustion chamber, they are assumed to belong to the radiation section for the sake of heat transfer calculations, i.e. Nr_{conv} does not include the shield tubes. Without loss of generality, we show the flow path of oil through the tubes in Fig. 6 for a specific set of passes and rows. Other furnace geometries have different geometries aimed at reducing the length of the path of the oil through the tubes.

Finally, the total height of the fired heater is given by:

$$H = H_{rad} + H_{conv} + H_s \tag{20}$$

Several additional geometric calculations related to the calculation of the heat transfer coefficient in the finned tubes of the convection section are shown later.

2.1. Radiant section

The radiation heat is related to the equivalent plane efficiency (α), the area of cold planes (A_{cp}), and the exchange factor (F) as follows.

$$Q_{rad}(1 - p\hat{Loss}_{rad}) = \alpha\, A_{cp}\, F\, \hat{\sigma}\,(T_{fb}^4 - T_w^4) + \hat{hcr} A_{rad}\,(T_{fb} - T_w) \tag{21}$$

where we consider that $Q_{rad}(1 - p\hat{Loss}_{rad})$ is the heat transferred through radiation and convection to the external wall of the tubes. In turn, $p\hat{Loss}_{rad}$ is an assumed percentage loss through the walls of the furnace (usually 2%). The equivalent plane efficiency (α), the exchange factor (F), the area of the cold plane (A_{cp}) and the external area of the tubes in the radiation section (including shield tubes) (A_{rad}) are given by (Mussati et al., 2009):

$$\alpha = \hat{c}_{\alpha,1}\left(\frac{d_c^{rad}}{d_o^{rad}}\right)^2 + \hat{c}_{\alpha,2}\left(\frac{d_c^{rad}}{d_o^{rad}}\right) + \hat{c}_{\alpha,3} \tag{22}$$

$$F = \hat{c}_{F,1} \ln(e_r) + (\hat{c}_{F,2} + \hat{c}_{F,3} e_r)\left\{\left(\left[\frac{2W_{rad}\, H_{rad} + 2E_l\,(W_{rad} + H_{rad})}{\hat{\alpha} A_{cp}}\right] - 1\right)\right\} + \hat{c}_{F,4} \exp(e_r) + \hat{c}_{F,5}\left\{e_r\left(\left[\frac{2W_{rad} \quad H_{rad} + 2E_l\,(W_{rad} + H_{rad})}{\hat{\alpha} A_{cp}}\right] - 1\right)\right\}^{1.5} + \hat{c}_{F,6} \tag{23}$$

$$(\alpha A_{cp}) = A_{cp}^{shield} + \alpha\, A_{cp}^{wall+ceil} \tag{24}$$

$$A_{rad} = Nt_{rad}\, \pi d_o^{rad}\, E_l \tag{25}$$

where:

$$A_{cp}^{Shield} = E_l\, Nt_{shield}\, d_c^{rad} \tag{26}$$

$$A_{cp}^{wall+ceil} = E_l\,(Nt_{rad} - Nt_{shield})\, d_c^{rad} \tag{27}$$

In turn, the flue gas emissivity is given by

$$e_r = \hat{c}_{e,1} T_{fb} + \hat{c}_{e,2} PL + \hat{c}_{e,3} PL^2 + \hat{c}_{e,4} \tag{28}$$

where PL is the product of the mean beam length and partial pressure of the CO_2 and H_2O.

$$PL = \left(\frac{2}{3}\right)(E_l\, W_{rad}\, H_{rad})^{1/3}\left[\hat{c}_{PL,1}(\hat{ex}_{air})^3 + \hat{c}_{PL,2}(\hat{ex}_{air})^2 + \hat{c}_{PL,3}\, \hat{ex}_{air} + \hat{c}_{PL,4}\right] \tag{29}$$

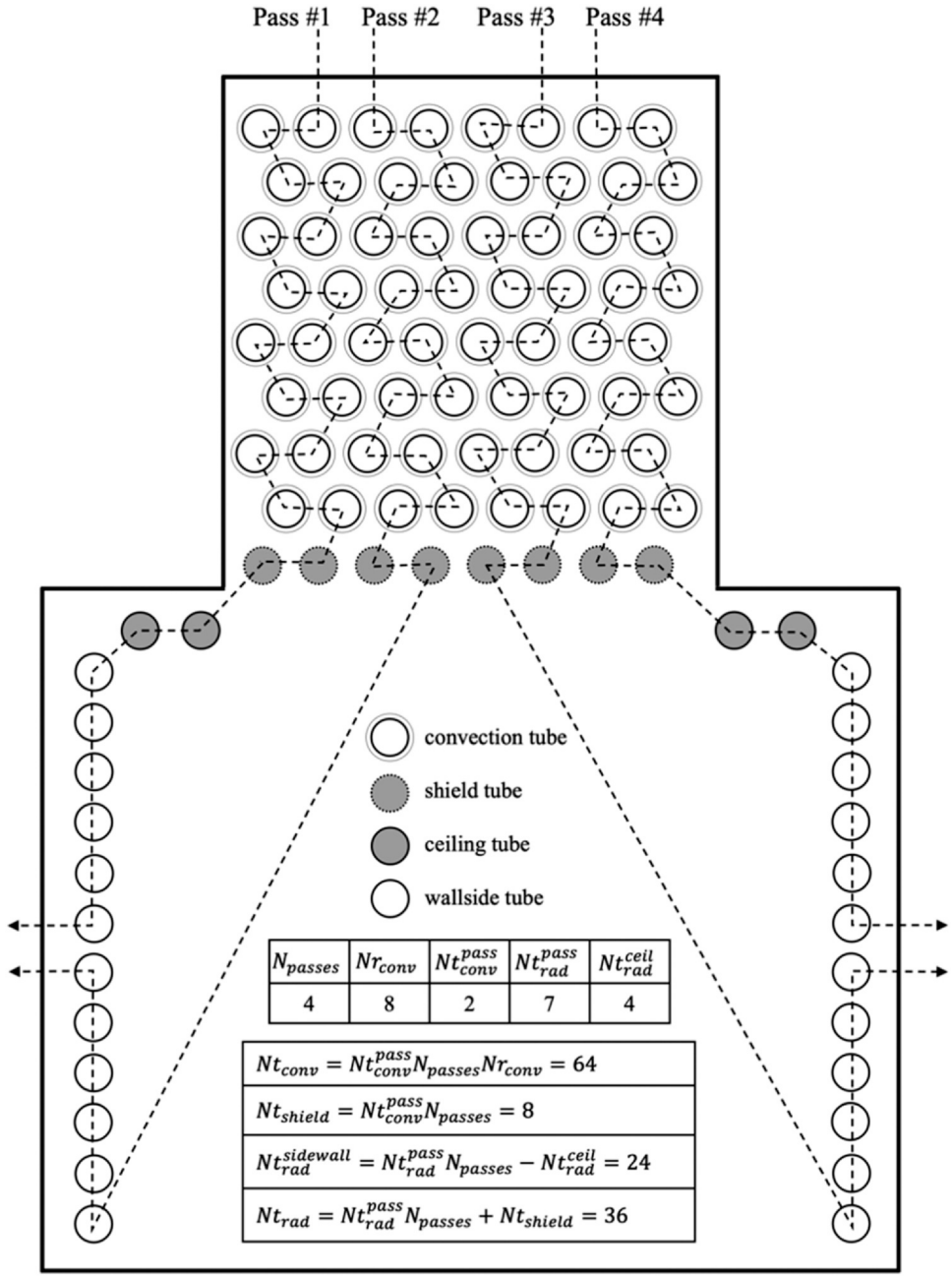

Fig. 6 – Distribution of the tubes inside a fired heater.

Note that the expressions for F and PL make use of the exposed length (E_l),rather than the full-fired heater length (L).

In turn, the natural convection coefficient ($\hat{hcr}$) on the outer surface of the tubes is not modeled and is assumed to be a constant parameter. The literature on fired heaters is void of attempts to model it and suggests using a constant value (Cao, 2009). The argument used is that it is a small part of the total heat transferred in the radiation section.

In addition, the heat transfer rate in the radiation section is equal to the heat absorbed by the oil, from its inlet temperature, T_c, to the outlet temperature, as follows:

$$Q_{Rad}\left(1 - p\hat{L}oss_{Rad}\right) = \hat{M}_{Oil}\left(\hat{h}_o^{oil} - \hat{co}_{h,1}(T_c)^2 - \hat{co}_{h,2}T_c - \hat{co}_{h,3}\right) \tag{30}$$

where $\hat{h}_o^{oil}$ is the enthalpy of the oil at the desired outlet temperature and $\hat{co}_{h,1}$, $\hat{co}_{h,2}$, and $\hat{co}_{h,3}$ are the coefficients for the enthalpy of the oil as a function of temperature. Indeed,

$$\hat{h}_o^{oil} = \hat{co}_{h,1}(\hat{T}_o)^2 + \hat{co}_{h,2}\,\hat{T}_o + \hat{co}_{h,3} \tag{31}$$

Note that T_c is the temperature of the oil entering the shield tubes, which are located in the convection section, but are considered part of the radiation section in the equations.

To complete the model, one needs to consider the heat transfer from the outside tube wall to the bulk of the oil. The corresponding (simplified) equation is:

$$Q_{rad}\left(1 - p\hat{L}oss_{rad}\right) = U_{rad,w}\,A_{rad}\left(T_w - \left(\frac{(\hat{T}_o + T_c)}{2}\right)\right) \tag{32}$$

where T_w is the temperature of the tube surface, and $U_{rad,w}$ is the overall heat transfer coefficient from the outside wall to the bulk of the fluid (flue gas fouling layer + wall conduction + oil fouling layer + inside convection). The temperature of the bulk is not local. Rather, we use an average between the

inlet and outlet temperature of the oil. The expression for evaluation of the overall heat transfer coefficient $U_{rad,w}$ is:

$$U_{rad,w} = \left(\frac{1}{\hat{Rf}_{gas} + \frac{d_o^{rad} \ln(d_o^{rad}/d_i^{rad})}{2\hat{k}_s} + \hat{Rft}_{max}\left(\frac{d_o^{rad}}{d_i^{rad}}\right) + \frac{1}{hct}\left(\frac{d_o^{rad}}{d_i^{rad}}\right)} \right) \quad (33)$$

where $\hat{k}_s$ is the thermal conductivity of the tube wall, $\hat{Rf}_{gas}$ is the fouling factor of the flue gas, $\hat{Rft}_{oil}$ is the fouling factor for the oil, hct is the inner side heat transfer coefficient, which we obtain using the Sieder-Tate correlation (without the correction associated with the viscosity variation) ($Nu = 0.023\,Re\,t^{0.8}\hat{Pr}^{0.33}$):

$$hct = 0.023\frac{\hat{k}_{oil}}{(d_i^{rad})^{1.8}}\left\{\frac{4\hat{M}_{Oil}}{N_{passes}\pi\,\hat{\mu}_{oil}}\right\}^{0.8}\hat{Pr}_{oil}^{0.33} \quad (34)$$

where $\hat{Pr}_{oil}$ and $\hat{k}_{oil}$ are the Prandtl number and the thermal conductivity of the oil stream.

We note that in the case of the model developed by Mussati et al. (2009), T_w is obtained by adding $\Delta\hat{t} = 100$ °F to the bulk inside tube average temperature, that is $T_w = (\hat{T}_o + T_c)/2 + \Delta\hat{t}$, an assumption we removed.

All the above equations for the radiation section contain non-geometry-related variables. When the geometry is fixed, the system of equations of the radiation section has one degree of freedom. This is of importance for the enumeration step that we will describe below.

2.2. Convection section

The heat transferred (Q_{conv}) in this section is related to the difference between the total heat absorbed by the oil, and is also related to heat transfer:

$$Q_{conv}(1 - p\hat{Loss}_{conv}) = \hat{M}_{Oil}(\hat{h}_o^{oil} - \hat{co}_{h,1}(\hat{T}_i)^2 - \hat{co}_{h,2}\hat{T}_i - \hat{co}_{h,3}) - Q_{rad}(1 - p\hat{Loss}_{rad}) \quad (35)$$

$$Q_{conv}(1 - p\hat{Loss}_{conv}) = U_{conv}A_{conv}LMTD \quad (36)$$

where A_{conv} is the heat transfer area of the convection section, that is,

$$A_{conv} = Nt_{conv}\,E_l\,Aot \quad (37)$$

where Aot is the finned surface area per unit length. In turn, LMTD is given by:

$$LMTD = [(T_{fb} - T_c) - (T_s - \hat{T}_i)]/\ln[(T_{fb} - T_c)/(T_s - \hat{T}_i)] \quad (38)$$

where T_s is the temperature of the flue gas leaving the convection section (i.e. the stack temperature) and T_{fb} is the temperature of the gas entering the convection section (after the shield tubes). These temperatures are related to the enthalpy variation of the flue gas in the radiation and convection sections:

$$M_{gas}\hat{Cp}_{gas}(\hat{T}_{flame} - T_{fb}) = Q_{rad}(1 - p\hat{Loss}_{rad}) \quad (39)$$

$$M_{gas}\hat{Cp}_{gas}(T_{fb} - T_s) = Q_{conv}(1 - p\hat{Loss}_{conv}) \quad (40)$$

where M_{gas} and $\hat{Cp}_{gas}$ are the mass flow rate and heat capacity of the flue gas. The heat capacity of the flue gas depends on the nature of the fuel and the excess air.

Finally, U_{conv} is obtained from the following set of equations (Cao (2009)):

$$U_{Conv} = \frac{1}{\left(\frac{1}{h_{Ci}^{HT}} + \hat{Rft}_{max}\right)\left(\frac{Aot}{\pi\ d_i^{rad}}\right) + \frac{Aot\ln\left(\frac{d_o^{conv}}{d_i^{conv}}\right)}{2\pi\ \hat{k}_t} + \frac{1}{\eta t\ h_{Co}^{HT}} + \frac{\hat{Rf}_{gas}}{\eta t}} \quad (41)$$

where h_{Ci}^{HT} and h_{Co}^{HT} are the convective heat transfer coefficients inside and outside the tubes, respectively, $\hat{k}t$ is the thermal conductivity of the tube wall, and ηt is the overall efficiency of the finned surface. In turn, the evaluation of the convective heat transfer coefficient inside the tubes also employs the Sieder-Tate correlation:

$$h_{Ci}^{HT} = 0.023\frac{\hat{k}_{oil}}{(d_i^{conv})^{1.8}}\left\{\frac{4\hat{M}_{Oil}}{N_{passes}\,\pi\,\hat{\mu}_{oil}}\right\}^{0.8}\hat{Pr}_{oil}^{0.33} \quad (42)$$

Next, the convective heat transfer coefficient for the flue gas flow around the finned surface is given by Cao (2009). Without loss of generality, we use a triangular layout:

$$h_{Co}^{HT} = j\ \hat{Cp}_{gas}\,G_{conv}\,\hat{Pr}_{gas}^{-0.67} \quad (43)$$

where $\hat{Pr}_{gas}$ is the Prandtl number of the flue gas and G_{conv} is the mass flux given by:

$$G_{conv} = \frac{M_{gas}}{A_s} \quad (44)$$

where A_s is the area of free flow across a center plane of a tube row, in turn, given by:

$$A_s = E_l\left\{W_{conv} - Nt_{conv}^{pass}N_{passes}\left[d_o^{conv} + N_f(d_f - d_o^{conv})t_f\right]\right\} \quad (45)$$

Next, Aot is given by:

$$Aot = Ab + Aof \quad (46)$$

where Ab is the exposed area of the root tube and Aof is the area of the fins, given by:

$$Ab = \pi d_o^{conv}(1 - t_f N_f) \quad (47)$$

$$Aof = \left[2\frac{\pi}{4}\left(d_f{}^2 - (d_o^{conv})^2\right) + \pi\ d_f\ t_f\right]N_f \quad (48)$$

The overall efficiency of the finned surface, ηt, depends on the fin efficiency (ηf):

$$\eta t = \left(\frac{Aot - Aof}{Aot}\right) + \eta f\left(\frac{Aof}{Aot}\right) \quad (49)$$

The fin efficiency can be calculated by:

$$\eta f = \frac{\tanh(mf \cdot l_{fe})}{mf \cdot l_{fe}} \quad (50)$$

$$mf = \sqrt{\left(\frac{2h'}{\hat{k}_{fin}\ t_f}\right)} \quad (51)$$

$$l_{fe} = l_f\left(1 + \frac{t_f}{2l_f}\right)\left[1 + 0.35\ln\left(\frac{d_f}{d_o^{conv}}\right)\right] \quad (52)$$

$$\frac{1}{h'} = \frac{1}{h_{Co}^{HT}} + \hat{Rf}_{gas} \quad (53)$$

where $\hat{k}_{fin}$ is the thermal conductivity of the fin.

Finally, the factor j for a triangular layout (ignoring the correction factor of the viscosity variation with temperature) is given by:

$$j = C_1 C_3 C_5 \left(\frac{d_f}{d_o^{conv}} \right)^{0.5} \tag{54}$$

$$C_1 = 0.091\,\mathrm{Re}^{-0.25} = 0.091 \left(\frac{d_o^{conv} \quad G_{conv}}{\hat{\mu}_{gas}} \right)^{-0.25} \tag{55}$$

$$C_3 = 0.35 + 0.65\exp\left[-\frac{0.125(d_f - d_o^{conv})}{s} \right] \tag{56}$$

$$C_5 = 0.7 + [0.7 - 0.8e^{-0.15(\mathrm{Nr}_{conv})^2}] e^{-\left(\frac{d_c^{conv,v}}{d_c^{conv,h}} \right)} \tag{57}$$

where s is the clearance between fins, given by:

$$s = \frac{1}{N_f} - t_f \tag{58}$$

We note that Eq. (54) is adapted from Cao (2009), which is presented with a temperature correction term based on the temperature of the gas divided by the temperature of the fin. This ratio is later assumed to be one in the example this author presented.

The above equations contain additional non-geometric variables to those already listed above for the radiation section. There are no degrees of freedom.

2.3. Stack

The fired heater analyzed in the current paper involves a natural draft. When designing, one needs to make sure that the draft provided by the stack and the firebox is larger than the sum of pressure drops, that is:

$$g(\hat{\rho}_{air} - \rho_{gas,avg})H \geq (1 + \varepsilon)(\hat{\Delta P}_b + \sum F) \tag{59}$$

where ε is a design margin for the draft evaluation, $\hat{\Delta P}_b$ is the pressure drop across the burner, a manufacturer value assumed here as a parameter, $\hat{\rho}_a$ is the density of the ambient air and $\rho_{gas,avg}$ is the average density of the flue gas along the fired heater, evaluated considering the flue gas density at the firebox temperature (T_{fb}) and the flue gas density leaving the stack (T_a), which can be evaluated considering a temperature decrease of 40 °C in the stack, as suggested by Cao (2009) (i.e. the temperature for the density evaluation at the heater outlet is T_s – 40 °C).

The friction losses are given by:

$$\sum F = \Delta p_{rad} + \Delta p_{conv} + \Delta p_{stack} + \Delta p_{minor} \tag{60}$$

where Δp_{rad}, Δp_{conv}, Δp_{stack}, and Δp_{minor} are the pressure drop in the radiation section, convection section, stack, and minor losses (stack entrance, stack outlet, and damper), respectively. The pressure drop across the firebox section is assumed negligible, that is, $\Delta p_{rad} \approx 0$. The pressure drop across the convection section is the pressure drop across the shield tubes plus the pressure drop across the finned tubes:

$$\Delta p_{conv} = \Delta p_{shield} + \Delta p_f \tag{61}$$

The pressure drop across the shield tubes is given by (according to Fig. 1, it is assumed a single row of shield tubes):

$$\Delta p_{shield} = 0.2 \frac{G_{shield}^2}{2\rho_{fb}} \tag{62}$$

where ρ_{fb} is the density of the gas at the temperature of the firebox (T_{fb}). G_{shield} is given by:

$$G_{shield} = \frac{M_{gas}}{A_{s,shield}} \tag{63}$$

where $A_{s,shield}$ is the area of free flow across a tube row of the shield tubes, given by:

$$A_{s,shield} = E_l \left\{ W_{conv} - Nt_{conv}^{pass} N_{passes}\, d_o^{conv} \right\} \tag{64}$$

The pressure drop across the finned horizontal tubes in the convection section is given by (Cao, 2009):

$$\Delta p_f = (f + a)\mathrm{Nr}_{conv} \frac{G_{conv}^2}{\rho_m} \tag{65}$$

$$a = \frac{1 + \beta^2}{4\,\mathrm{Nr}_{conv}} \rho_m \left(\frac{1}{\rho_{fb}} - \frac{1}{\rho_s} \right) \tag{66}$$

$$\beta = \frac{A_s}{W_{conv} E_l} \tag{67}$$

where ρ_s is the density of the gas at the convection section outlet (T_s), and ρ_m is the mean density of the flue gas in the convection section. Without loss of generality, we calculate this mean density by using the average temperature, instead of taking the average of densities. The friction factor in Eq. (67) is evaluated by:

$$f = C_2 C_4 C_6 \left(\frac{d_f}{d_o^{conv}} \right) \tag{68}$$

where the different coefficients are given by:

$$C_2 = 0.075 + 1.85\,\mathrm{Re}^{-0.3} = 0.075 + 1.85 \left(\frac{d_o^{conv} \; G}{\hat{\mu}_{gas}} \right)^{-0.3} \tag{69}$$

$$C_4 = 0.11 \left(0.05 \frac{d_c^{conv,h}}{d_o^{conv}} \right)^m \tag{70}$$

$$m = -0.7 \left(\frac{l_f}{s} \right)^{0.2} \tag{71}$$

$$C_6 = 1.11 + \left[1.8 - 2.1e^{-0.15N_f^2} \right] e^{-2\left(\frac{d_c^{conv,v}}{d_c^{conv,h}} \right)} - \left[0.7 - 0.8e^{-0.15N_f^2} \right] e^{-0.6\left(\frac{d_c^{conv,v}}{d_c^{conv,h}} \right)} \tag{72}$$

In these equations, the correction for fin temperature is not included although Cao (2009) uses that but later ignores it in his examples. Finally, the pressure drop in the stack is:

$$\Delta p_{stack} = 2.76 \cdot 10^{-5} \left(\frac{G_{stack}^2 T_{stack}}{D_s} \right) H_s \tag{73}$$

where D_s is the stack diameter, G_{stack} is the mass flux of the flue gas in the stack (kg/(s·m^2)), and T_{stack} is the mean temperature of the flue gas throughout the stack. This mean temperature is recommended to be based on assuming a temperature variation of 40 °C throughout the stack (Cao, 2009). The stack mass flux is given by:

$$G_{stack} = \left(\frac{M_{gas}}{\frac{\pi D_s^2}{4}} \right) \tag{74}$$

The minor losses associated with the flow along the stack are given by:

$$\Delta p_{minor} = 3 \frac{G_{stack}^2}{2\rho_{stack}} \tag{75}$$

where ρ_{stack} is the mean density of the gas throughout the stack.

2.4. Inequality constraints

The following geometric constraints (heuristics from practice) for the radiant box are (Mussati et al., 2009):

$$1 \le \frac{H_{rad}}{W_{rad}} \le 1.5 \tag{76}$$

$$1.8 \le \frac{L}{W_{rad}} \le 3 \tag{77}$$

Now, a rough guide to the radiant box size ($E_l\ W_{rad}\ H_{rad}$) is a ratio of volume over the radiant transfer area ($\pi\ d_o\ E_l\ Nt^{rad}$) to have enough space to avoid flame impingement on the tubes. The following constraint reflects the accepted range.

$$3.5 \le \frac{W_{rad} H_{rad}}{\pi d_o^{rad}\, Nt_{rad}} \le 4.5 \tag{78}$$

The geometric constraints for the whole fired heater are:

$$H < H_{Max} \tag{79}$$

$$D_s < W_{conv} \tag{80}$$

The geometric constraints for the radiation tubes are:

$$d_c^{rad} \ge d_o^{rad} + \hat{\varepsilon}_r \tag{81}$$

where $\hat{\varepsilon}_r$ is a mandatory minimum separation between tubes.

The geometric constraints for the finned tubes are:

$$d_c^{conv,h} \ge 2l_f + d_o^{conv} \tag{82}$$

$$\sqrt{(d_c^{conv,v})^2 + \left(\frac{d_c^{conv,h}}{2}\right)^2} \ge 2l_f + d_o^{conv} \tag{83}$$

Limits on velocities and pressure drop inside the tubes:

$$V_{oil}^{tube,rad} = \frac{\hat{M}_{oil}}{N_{passes}\hat{\rho}_{oil}\,[\pi\,(d_i^{rad})^2/4]} \le V_{oil,MAX}^{tube} \tag{84}$$

$$V_{oil}^{tube,conv} = \frac{\hat{M}_{oil}}{N_{passes}\hat{\rho}_{oil}\,[\pi\,(d_i^{conv})^2/4]} \le V_{oil,MAX}^{tube} \tag{85}$$

$$\Delta P_{oil}^{tube,rad} + \Delta P_{oil}^{tube,conv} = \left(\frac{L_{oil}\hat{\rho}_{oil}}{2}\right)\left(\frac{f_{rad}\,(V_{oil}^{tube,rad})^2}{d_i^{rad}} + \frac{f_{conv}\,(V_{oil}^{tube,conv})^2}{d_i^{conv}}\right) \le \Delta P_{oil,Max}^{tube} \tag{86}$$

where the velocity limit is to prevent erosion, while the limit on pressure drop is related to maximum assumed pumping costs. One can easily add these pumping costs to the total annualized cost and eliminate the pressure drop constraint (unless there are some other additional limitations stemming from other issues than pumping cost). In the above equations, the friction factors are obtained as follows (Asker et al., 2014):

$$f_{rad} = 5.5 \times 10^{-3}\left[1 + \left(2 \times 10^4\left(\frac{\hat{r}}{d_i^{rad}}\right) + \frac{10^6}{Re_t^{rad}}\right)^{1/3}\right] \tag{87}$$

$$f_{conv} = 5.5 \times 10^{-3}\left[1 + \left(2 \times 10^4\left(\frac{\hat{r}}{d_i^{conv}}\right) + \frac{10^6}{Re_t^{conv}}\right)^{1/3}\right] \tag{88}$$

where $\hat{r}$ is the roughness of the tubes, while Re_t^{rad} and Re_t^{conv} are the Reynolds numbers in the tubes, given by:

$$Re_t^{rad} = \frac{4\hat{M}_{Oil}}{d_i^{rad} N_{passes}\pi\,\hat{\mu}_{oil}} \tag{89}$$

$$Re_t^{conv} = \frac{4\hat{M}_{Oil}}{d_i^{conv} N_{passes}\pi\,\hat{\mu}_{oil}} \tag{90}$$

Limits on the firebox temperature:

$$\hat{T}_{fb,\min} \le T_{fb} \le \hat{T}_{fb,\max} \tag{91}$$

The maximum value is related to material issues and the minimum value is extracted from industrial practice.

The limits on the flux in the firebox:

$$Flux_{Min} \le Flux \le Flux_{Max} \tag{92}$$

where the flux is defined by:

$$Flux = \frac{Q_{rad}}{A_{rad}} \tag{93}$$

The above minimum value for flux is connected to heuristics that come from industrial practices, and the maximum value is related to tube wall material issues.

Limits established for the mass flux of gases across the shield tubes in the convection section (Couper et al., 2012):

$$G_{shield,Min} \le G_{shield} \le G_{shield,Max} \tag{94}$$

which are rooted in heuristics used in industry; the higher limit is likely associated with erosion velocities, and the lower one is a way to avoid low heat transfer.

Limits on the stack temperature:

$$\hat{T}_{s,\min} \le T_s \tag{95}$$

The lower limit may be imposed to avoid the acid dew point temperature, thus protecting the fired heater from the formation of acid condensation.

Finally, the draft inequality in Eq. (61) holds.

2.5. Cost equations

We use the following equations, adapted from Mussati et al. (2009) for the total annualized cost (TAC) that encompasses the costs of the radiant coil (R_{cost}), convection coil (C_{cost}), firebox (FB_{cost}), stack (St_{cost}) and operating costs (O_{cost}), as expressed below:

$$TAC = R_{cost} + C_{cost} + FB_{cost} + St_{cost} + O_{cost} \tag{96}$$

where:

$$R_{cost} = \hat{r}_{cost} A_{rad} C\hat{R}F \tag{97}$$

$$C_{cost} = \hat{c}_{cost} A_{conv} C\hat{R}F \tag{98}$$

$$FB_{cost} = [\hat{k}1 + \hat{k}2(A_{rad} + A_{conv})]\,C\hat{R}F \tag{99}$$

$$St_{cost} = \hat{s}_{cost}\, H_s\, \pi\, D_s\, t_s\, C\hat{R}F \tag{100}$$

$$O_{cost} = \hat{fuel}_{cost}\, M_{fuel} O\hat{T} \tag{101}$$

where t_s is the stack wall thickness and M_{fuel} is the fuel flowrate given by:

$$M_{fuel} = Q_n/LHV \tag{102}$$

In turn, Q_n is the total heat released by the fuel burnt, which is equivalent to the heat transfer in the radiation section, the convection section, and the stack losses:

$$Q_n = Q_{rad} + Q_{conv} + Q_s \tag{103}$$

where:

$$Q_s = M_{gas}\, Cp_{gas}\,(T_s - \hat{T}_a) \tag{104}$$

In the above equations $\hat{r}_{cost}$, $\hat{c}_{cost}$, $\hat{s}_{cost}$, and $\hat{fuel}_{cost}$ are the unitary radiation tube cost, the unitary convection tube cost, the stack material cost per unit weight, and the fuel cost, respectively. In turn, $\hat{CRF}$ is the annualization factor and $\hat{OT}$ is the number of hours per year of operation. Finally $\hat{k1}$ and $\hat{k2}$ are cost parameters that depend on the type of refractory, coil materials, insulation width, etc.

3. Basic design problem

The basic design of the fired heater can be defined as follows: given the flow rate and composition of the fluid to be heated, the type of fuel to be used, the excess air (without loss o generality, this is fixed here, and it determines the flame temperature and the flue gas flowrate; it can be optimized), the type of fired heater, and corresponding limits on key dimensions and operating values of key variables (flows, temperatures, heat fluxes, etc.) determine the dimensions such that the heating task is achieved and the cost is minimum.

In this article, we limit the search to:

- Box-type fired heater.
- Natural draft.
- Natural gas as fuel.
- Only one circular stack is located above the convection section.

Thus, the following outcomes are expected at the end of the design (related to the independent variables listed in Section 2 of the current paper):

- Radiation section dimensions (length, width, and height)
- Convection section dimensions (length, width, and height)
- Number of tubes in the ceiling and sidewalls of the radiation section
- Number of shield tubes
- Number of tube rows in the convection section and number of tubes in each row
- Stack diameter and height.
- Number of passes
- Tube diameter and thickness in the radiation and convection sections
- Feature of the finned surface in the convection section (fin height, fin thickness and number of fins per unit length)
- Fuel flowrate

In addition, several other property values that stem from the use of the above variables are determined: temperatures, flows, pressure drops, heat flux, etc., that is, all values of interest.

The model has certain degrees of freedom, so the design can be approached by selecting different sets of independent variables and optimizing varying them.

Many geometric variables are naturally discrete, such as the number of tubes in each section of the furnace. Some other geometric variables are discrete because of fabrication issues, such as tube diameters, tube wall thickness, etc. Finally, other variables, such as the length of tubes, which can be thought of as continuous, need to be expressed in discrete ways (to a fraction of inches, for example), amenable for blueprints in detailed engineering.

Despite the discrete nature of the geometric variables, it has been the practice of several design methods to treat certain geometric variables as continuous variables to later round up to the next discrete value available commercially. Presumably, this approach was popularized by the idea that binary variables ought to be avoided and nonlinear problems are easier to handle. We choose the former approach of using discrete values because it is more accurate and does not introduce any computational issues.

4. Set Trimming

This procedure consists of generating a set of candidates, described by a combination of all the independent discrete variables of the system, followed by a trimming routine to reduce the candidate pool using the problem inequality constraints (Costa and Bagajewicz, 2019). We also use proxy constraints, which are based on using limiting values of variables. Thus, if a candidate does not satisfy the bound, it is eliminated.

We now present the Set Trimming steps, some using the inequalities of the problem directly and some others using proxy constraints.

- *Set Trimming for Geometry:*
  Test and eliminate the candidates that violate the set of constraints associated with the fired heater geometry. These tests are applied according to the established order (only feasible candidates filtered by previous constraints are tested, so there is a reduction of the computational effort). Equations (76–83) are used for the geometric set trimming.

- *Set Trimming for Oil Velocity and Pressure Drop:*

The set of trimming related to the velocity and pressure drop bounds are: Eqs. (84–86).

- *Proxy Set Trimming for Mass Flux of Gas:*

Because it is not possible to obtain G without solving the whole model, which is expensive computationally, we resort to using extreme values of it, which can be tested on all surviving candidates through a low computational effort. To do that, it is required to obtain the upper/lower bounds of the radiation section heat transfer rate. They are obtained from the maximum/minimum heat flux:

$$Q_{rad}^{UB}\,(1 - \hat{pLoss}_{rad}) = \hat{Flux}_{MAX}\, A_{rad} \tag{105}$$

$$Q_{rad}^{LB}\,(1 - \hat{pLoss}_{rad}) = \hat{Flux}_{MIN}\, A_{rad} \tag{106}$$

The upper/lower bounds of the gas mass flowrate and mass flux are as follows:

$$M_{gas}^{LB} = \frac{Q_{rad}^{LB}\,(1 - \hat{pLoss}_{rad})}{\hat{Cp}_{gas}\,(\hat{T}_{flame} - \hat{T}_{fb}^{MIN})} \tag{107}$$

$$M_{gas}^{UB} = \frac{Q_{rad}^{UB}\,(1 - \hat{pLoss}_{rad})}{\hat{Cp}_{gas}\,(\hat{T}_{flame} - \hat{T}_{fb}^{MAX})} \tag{108}$$

$$G_{LB} = \frac{M_{gas}^{LB}}{A_s} \tag{109}$$

$$G_{UB} = \frac{M_{gas}^{UB}}{A_s} \tag{110}$$

Based on these bounds, the following Proxy Set Trimmings can be applied:

- Testing $G \le G_{MAX}$ through a Proxy relation. If $G_{LB} > G_{MAX}$, eliminate these candidates.
- Testing $G \ge G_{MIN}$ through a Proxy relation. If $G_{UB} < G_{MIN}$, eliminate these candidates.

- *Proxy Set Trimming for the Radiation Section:*

We now use extreme values of the heat flux and obtain limits for the inlet oil temperature of the shield tubes (T_c) and the firebox temperature (T_{fb}). The upper/lower bounds of T_c are obtained using the upper/lower bound of the radiation section heat rate.

$$Q_{rad}^{UB}(1 - pL\hat{o}ss_{rad}) = \hat{M}_{Oil}(\hat{h}_o^{oil} - \hat{co}_{h,1}(T_c^{LB})^2 - \hat{co}_{h,2}T_c^{LB} - \hat{co}_{h,3}) \quad (111)$$

$$Q_{rad}^{LB}(1 - pL\hat{o}ss_{rad}) = \hat{M}_{Oil}(\hat{h}_o^{oil} - \hat{co}_{h,1}(T_c^{UB})^2 - \hat{co}_{h,2}T_c^{UB} - \hat{co}_{h,3}) \quad (112)$$

- Testing $T_c < \hat{T}_{fb,Max} - \Delta\hat{T}_{\min}$. Here $\Delta\hat{T}_{\min}$ is the minimum temperature approach, (we use 5 °C, but the literature recommends higher values; in such a case, set trimming with eliminate more candidates). If $T_c^{LB} > \hat{T}_{fb,Max} - \Delta\hat{T}_{\min}$, the candidate is eliminated.
- Testing $T_c > \hat{T}_i$, a natural constraint that is implicit in the model. If $T_c^{UB} < \hat{T}_i$, the candidate is eliminated.
  In turn, the upper/lower bounds of the firebox temperature are calculated using the upper/lower bound of the gas mass flowrate and heat transfer rate.

$$M_{gas}^{LB}(\hat{Cp}_{gas}(\hat{T}_{flame} - T_{fb}^{LB})) = Q_{rad}^{UB}(1 - pL\hat{o}ss_{rad}) \quad (113)$$

$$M_{gas}^{UB}(\hat{Cp}_{gas}(\hat{T}_{flame} - T_{fb}^{UB})) = Q_{rad}^{LB}(1 - pL\hat{o}ss_{rad}) \quad (114)$$

- Testing $T_{fb} < \hat{T}_{fb,\max}$. If $T_{fb}^{LB} > \hat{T}_{fb,\max}$, eliminate these candidates.
- Testing $T_{fb} > \hat{T}_{fb,\min}$. If $T_{fb}^{UB} < \hat{T}_{fb,\min}$, eliminate these candidates. It has an exit temperature too high, even under minimum flux conditions.
- If $T_{fb}^{UB} < T_c^{LB}$, eliminate these candidates.

- *Proxy Set Trimming for the Convection Section:*

We first obtain two types of lower and upper bounds of the convection section heat transfer rate (Q_{conv}^{LB1}, Q_{conv}^{UB1}) as well as (Q_{conv}^{LB2}, Q_{conv}^{UB2}). The first set is obtained from heat transfer considerations and the second set is obtained using the upper and lower bounds of the radiation section, as follows:

$$Q_{conv}^{LB1}(1 - pL\hat{o}ss_{conv}) = U_{LB}A_{conv}LMTD_{LB} \quad (115)$$

$$Q_{conv}^{UB1}(1 - pL\hat{o}ss_{conv}) = U_{UB}A_{conv}LMTD_{UB} \quad (116)$$

$$Q_{conv}^{LB2}(1 - pL\hat{o}ss_{conv}) = \hat{M}_{Oil}(\hat{h}_o^{oil} - \hat{co}_{h,1}(\hat{T}_i)^2 - \hat{co}_{h,2}\hat{T}_i - \hat{co}_{h,3}) - Q_{rad}^{UB} \quad (117)$$

$$Q_{conv}^{UB2}(1 - pL\hat{o}ss_{conv}) = \hat{M}_{Oil}(\hat{h}_o^{oil} - \hat{co}_{h,1}(\hat{T}_i)^2 - \hat{co}_{h,2}\hat{T}_i - \hat{co}_{h,3}) - Q_{rad}^{LB} \quad (118)$$

The expressions for the upper and lower bounds used in Eqs. (115 and 116) are shown in Supplemental Material S1.

- Testing $T_s > \hat{T}_i + \Delta\hat{T}_{\min}$. If $T_s^{UB} < \hat{T}_i + \Delta\hat{T}_{\min}$ (i.e. the gas temperature is smaller than the inlet temperature plus a minimum approach $\Delta\hat{T}_{\min}$), then the candidate is eliminated. Supplemental Material S1 shows the bounds on T_s.
- Testing $T_s < T_{fb}$.If $T_s^{LB} > T_{fb}^{UB}$, that is, if the lower bound on the temperature of the gas leaving the convection section is higher than the upper bound on the firebox temperature, then eliminate this candidate.
- If $\min(Q_{conv}^{UB1}, Q_{conv}^{UB2}) < \max(Q_{conv}^{LB1}, Q_{conv}^{LB2})$, the candidate for the upper bound on the heat transfer rate in the convection section based on transport equations does not reach the convection section heat load calculated using the upper bound of the radiation section heat load, then eliminate the candidate.

- *Set Trimming for the Stack Section:*

The Proxy Set Trimming used here is based on using bounds on the different terms of the friction losses ($\sum F_{LB}$) in the draft inequality constraint. The corresponding bounds are described in Supplemental Material S2.

- Testing $g(\rho_{air} - \rho_{gas,avg})H \ge (1 + \varepsilon)(\Delta\hat{P}_b + \sum F)$. If $g(\rho_a - \rho_{g,o})H < (1 + \varepsilon)(\Delta\hat{P}_b + \sum F^{LB})$, eliminate the candidate. Here $\rho_{g,o}$ is the density of the flue gas at its minimum value, which corresponds to the flame temperature in the burner.

It is important to observe that the tests and eliminations presented above that compose the Set Trimming procedure are not applied for individual candidates, using computational loops (e.g. “for” loops). Set Trimming is based on the use of specialized computational routines associated with the handling of sets of data.

5. Smart Enumeration

As stated above, in Smart Enumeration, all candidates remaining after the Set Trimming steps are first organized in increasing order of the lower bound of their objective function. Next, they are evaluated rigorously one by one, starting with the candidate with the lowest value of the lower bound. If a candidate is feasible and its cost is smaller than the incumbent candidate’s cost, it becomes the new incumbent. The enumeration stops when the candidate’s objective function lower bound is larger than the incumbent’s cost. The detailed evaluation of the lower bound of the objective function and the feasibility test steps are shown below. The enumeration steps are the following:

- Calculate the cost of the first candidate from its geometry. This requires solving the set of equations that are

summarized in Supplemental Material S3. The solution of this system of equations is unique (Supplemental Material S5).

- If the first candidate is feasible, this is the first incumbent.
- Go to the next candidate according to the ascending order of the objective function lower bound.
- If the candidate is feasible and its objective function is lower than the incumbent objective function, then this is the new incumbent, otherwise, the first incumbent stays.
- If the next candidate has an objective function lower bound higher than the objective function of the incumbent, stop. The solution has been found.
- Go to Step [3].

The Smart Enumeration algorithm is presented in a flowchart form in the Supplemental Material S4.

6. Lower bounds for Smart Enumeration

- Calculate the lower bound of the amount of heat lost in the stack (Q_s^{LB}).

$$Q_s^{LB} = M_{gas}^{LB} \quad cpg_1 \quad (\hat{T}_i - \hat{T}_a) \tag{121}$$

- Calculate the lower bound of the total heat transferred to the oil plus the stack loss (Q_n^{LB}).

$$Q_n^{LB} = Q_{rad}^{LB} + Q_{conv}^{LB} + Q_s^{LB} = Q_{rad}^{LB} + (Q_{oil} - Q_{rad}^{UB}) + Q_s^{LB} \tag{122}$$

- Calculate the lower bound of the amount of fuel (M_f^{LB}).

$$M_f^{LB} = Q_n^{LB}/LHV \tag{123}$$

- Calculate the lower bound of the operating cost using the minimum amount of fuel

$$O_{cost}^{LB} = \hat{fuel} M_f^{LB} \hat{OT} \tag{124}$$

- Obtain the lower bound of the total cost

$$T_{cost}^{LB} = R_{cost} + C_{cost} + FB_{cost} + S_{cost} + O_{cost}^{LB} \tag{125}$$

7. Feasibility test

Once the model is solved rigorously for any fixed geometry, its viability is checked using the Eqs. (59), (92), and (94).

8. Results

The Set Trimming and Smart Enumeration method was implemented in GAMS to obtain the globally optimal solutions for the design of fired heater examples. Instead of using the "LOOP" or "FOR" features in GAMS to inspect one candidate at a time, we use "Dynamic Sets", which trims the set using the corresponding condition inspecting all candidates simultaneously. Three different flowrates of oil were considered, with the same initial and final temperatures (see Table 1). The model parameters are shown in Table 2. The discrete options of the independent design variables are shown in Table 3. Note that the tube diameters (d_o^{rad} and d_o^{conv}) are considered to be equal and, together with the wall thickness (t_d), which are also equal, come in pairs using Schedule 40.

The optimal fired heater obtained in each example is shown in Tables 4 and 5. Some optimal values of the variables are located at a search space bound (e.g. Nr_{conv}). Some of these bounds were based on Mussati et al. (2019), but they are a designer decision and any set of discrete values can be selected for building the search space.

Table 1 – Example data used in the case studies.

Parameter		values
Oil mass flow rate (lb/s) (kg/s)	Example 1	99.16 – 44.98
	Example 2	71.39 – 32.38
	Example 3	126.94 – 57.58
Oil inlet temperature (°F) (K)		380 – 466
Oil outlet temperature (°F) (K)		675 – 357

Table 2 – Model parameters.

Parameters	Value
$\hat{\rho}_{oil}$ (lb/ft^3) (kg/m^3)	44.3594 – 710.57
$\hat{\rho}_a$ (lb/ft^3) (kg/m^3)	0.0765 – 1.2254
$\hat{cpg}_1$ (Btu/lb·°F) (J/kg·K)	0.340– 1423.512
$\hat{perc}Loss_{Rad}$	0.02
$\hat{perc}Loss_{Conv}$	0.02
$\hat{co}_{h,1}$	0.0004208148
$\hat{co}_{h,2}$	0.2679048
$\hat{co}_{h,3}$	110.4305
$\hat{c}_{F,1}$	0.325
$\hat{c}_{F,2}$	0.215
$\hat{c}_{F,3}$	-0.073
$\hat{c}_{F,4}$	0.07
$\hat{c}_{F,5}$	-0.049
$\hat{c}_{F,6}$	0.594
$\hat{\sigma}$ (Btu/s·ft^2·R^4) (W/m^2·K^4)	$4.7611\cdot10^{-13}$ – $5.67\cdot10^{-8}$
$\hat{hcr}$ (Btu/hr·ft^2·°F) (W/m^2·K)	7 – 39.75
$\hat{h}_o^{oil}$ (Btu/lb) (J/kg)	483 – $1.1234\cdot10^6$
$\hat{h}_{flame}^{gas}$ (Btu/lb) (J/kg)	1075.0673 – $2.5006\cdot10^6$
$\hat{k}_s$ (Btu/ft·s·F) (W/m·K)	0.0025694 – 15.9983
$\hat{k}_{oil}$ (Btu/ft·s·F) (W/m·K)	0.0000193 – 0.1202
$\hat{k}_{fin}$ (Btu/ft·s·F) (W/m·K)	0.0073075 – 45.4999
$\hat{k}_t$ (Btu/ft·s·F) (W/m·K)	0.0073075 – 45.4999
$\hat{\mu}_{gas}$ (lb/ft·s) (kg/m·s)	$3.25233\cdot10^{-5}$ – $4.8400\cdot10^6$
$\hat{\mu}_{Oil}$ (lb/ft·s) (kg/m·s)	0.00552 – 0.00821
$\hat{Rft}_{max}$ (s·ft^2·°F/Btu) (m^2·K/W)	20.44 – $9.9991\cdot10^{-4}$
$\hat{Rfgas}$ (s·ft^2·°F/Btu) (m^2·K/W)	18.00 – $8.8055\cdot10^{-4}$
Excess air (%)	15
$\hat{\Delta P}_b$ (in H_2O) (mm H_2O)	0.5 – 12.70
ε	0.05
LHV (Btu/lb) (J/kg)	21500 – $5.0009\cdot10^7$
$\hat{r}_{cost}$ ($/ft^2) ($/m^2)	170 – 1829.86
$\hat{c}_{cost}$ ($/ft^2) ($/m^2)	100 – 1076.39
$\hat{s}_{cost}$($/ft^3) ($/m^3)	111 – 1194.79
$\hat{fuel}_{cost}$ ($/lb) ($/kg)	0.043 – 0.0948
$\hat{k1}$ ($)	5000
$\hat{k2}$ ($/ft^2) ($/m^2)	50 – 538.195
$\hat{CRF}$	0.18
$\hat{OT}$ (hr/yr)	8000 – 0.9132

Table 3 – Discrete options of independent design variables.

Design variables	Discrete options
L (ft) (m)	{30, 35, 40, 45, 50} – { 9.14, 10.67, 12.19, 13.72, 15.24}
(d_o, t_d) (ft) (m)	{(0.2917, 0.0183), (0.3333, 0.0192), (0.3750, 0.0200), (0.4636, 0.0217), (0.5521, 0.0233)} – {(0.0889,0.0056), (0.1016,0.0058), (0.1143,0.0061), (0.1413,0.0066), (0.1683,0.0071)}
N_{passes}	8, 10, 12, 14, 16
Nt_{rad}^{ceil}	10, 12, 14, 16, 18
Nr_{conv}	8, 9, 10, 11, 12
Nt_{rad}^{pass}	8, 9, 10, 11, 12
Nt_{conv}^{pass}	1, 2, 3, 4
H_s (ft) (m)	50, 60, 70, 80 – 15.24, 18.29, 21.34, 24.38
(D_s, t_s) (ft) (m)	{(3, 0.1667), (6, 0.250), (9, 0.333)}– {(0.9144,0.0508), (1.8288,0.0762), (2.7432,0.1015)}
r_p^{rad}	1.80, 1.85, 1.90, 1.95
$r_p^{conv,h}$	1.55, 1.60, 1.65
$r_p^{conv,v}$	1.45
(d_o, t_f, l_f, N_f) (ft) (m)	{(0.2917, 0.00905, 0.0833, 48), (0.3333, 0.00905, 0.0833, 48), (0.3750, 0.00905, 0.0833, 48), (0.4636, 0.00905, 0.0833, 48), (0.5521, 0.00905, 0.0833, 48)}– {(0.0889,0.0027,0.0254,48), 0.1016,0.0027,0.0254,48), 0.1143,0.0027,0.0254,48), 0.1413,0.0027,0.0254,48), 0.1683,0.0027,0.0254,48)}

Table 4 – Optimal Heater.

	Example 1	Example 2	Example 3
Total cost ($)	2,719,482.3	2,082,403.3	3,473,901.8
Q_n (Btu/s) (MW)	14,055.8 – 14.83	9,585.1 – 10.12	17,069.7 – 18.01
Q_{rad} (Btu/s) (MW)	7,194.2 – 7.59	5,712.6 – 6.03	10,132.7 – 10.69
Q_{conv} (Btu/s) (MW)	7,245.9 – 7.64	7,238.7 – 7.64	10,340.3 – 10.91
Q_s (Btu/s) (MW)	28,495.9 – 30.06	22,536.4 – 23.78	37,542.7 – 39.61
T_{fb} (°F) (K)	1,766.6 – 1236.8	1,992.7 – 1362.4	1,894.6 – 1307.9
T_w (°F) (K)	1,395.0 – 1030.4	1,681.8 – 1189.7	1,505.4 – 1091.7
T_c (°F) (K)	492.0 – 528.7	502.7 – 534.7	502.4 – 534.5
T_s (°F) (K)	933.4 – 773.9	1,157.3 – 898.3	1,004.2 – 813.3
M_{gas} (lb/s) (kg/s)	24.9125 – 11.3001	19.7291 – 8.9490	32.8357 – 14.8940
M_{fuel} (lb/s) (kg/s)	1.3254 – 0.6012	1.0482 – 0.4755	1.7462 – 0.7921
G_{conv} (lb/ft^2·s) (kg/m^2·s)	0.3867 – 1.8880	0.3773 – 1.8421	0.3930 – 1.9188
e_r	0.5357	0.4754	0.5254
LMTD (°F) (K)	864.4 – 735.6	1,095.2 – 863.8	957.4 – 787.3
h_{Co}^{HT} (Btu/ft^2·s·°F) (W/m^{2}K)	0.0010 – 20.4417	0.0010 – 20.4417	0.0010 – 20.4417
F	0.6411	0.6156	0.6337
ηt	0.9192	0.9200	0.9178
ηf	0.9148	0.9156	0.9133
mf	5.3814	5.3540	5.4352
h'(Btu/ft^2·s·°F) (W/m^2·K)	0.0010 – 20.4417	0.0009 – 18.3976	0.0010 – 20.4417
j	0.0061	0.0062	0.0061
O_{cost} ($)	1,641,363.9	1,298,093.8	2,162,459.0
U_{conv} (Btu/ft^2·s·°F) (W/m^2·K)	0.0002 – 4.0883	0.0002 – 4.0883	0.0003 – 6.1325

The progression of the Set Trimming, the number of simulations employed during the Smart Enumeration and the computational times of the complete procedure are shown in Table 6. The optimization runs were executed in a computer with 3.2 GHz 8 Core Intel Xeon W CPU and 32 GB RAM.

The results depicted in Table 6 indicate that the Set Trimming procedure was very effective in the reduction of the number of candidates. At the end of this procedure the remaining candidates are only a small fraction of the search space. The number of candidates after the Set Triming procedure in each example corresponds to only 0.086%, 0.054% and 0.025% of the initial search space.

It should be observed that the Smart Enumeration also contributed to the computational performance of the algorithm. After the Set Trimming, the global optimum is identified through the solution of the complete model of only a small number of solution candidates: 5.77%, 5.33% and 9.82% of the number of remaining candidates after Set Trimming.

Table 5 – Optimal Heater Geometry.

	Base case	Smaller case	Larger case
L (ft) (m)	40 – 12.19	30 – 9.14	40 – 12.19
d_o^{rad} (ft) (m)	0.3750 – 0.1143	0.3750 – 0.1143	0.3750 – 0.1143
t_d (ft) (m)	0.0200 – 0.0061	0.0200 – 0.0061	0.0200 – 0.0061
N_{passes}	8	8	10
Nt_{rad}^{ceil}	18	14	18
Nr_{conv}	8	8	8
Nt_{rad}^{pass}	12	10	10
Nt_{conv}^{pass}	1	1	1
H_s (ft) (m)	50 – 15.24	50 – 15.24	80 – 24.38
D_s (ft) (m)	3 – 0.9144	3 – 0.9144	3 – 0.9144
t_s (ft) (m)	2/12 – 0.0508	2/12 – 0.0508	2/12 – 0.0508
r_p^{rad}	1.90	1.95	1.80
$r_p^{conv,h}$	1.60	1.65	1.65
$r_p^{conv,v}$	1.45	1.45	1.45
d_o^{conv} (ft) (m)	0.3750 – 0.1143	0.3750 – 0.1143	0.3750 – 0.1143
t_f (ft) (m)	0.00905 – 0.0027	0.00905 – 0.0027	0.00905 – 0.0027
lf (ft) (m)	0.0833 – 0.0254	0.0833 – 0.0254	0.0833 – 0.0254
Nf	48	48	48
d_c^{rad} (ft) (m)	0.675 – 0.206	0.731 – 0.223	0.675 – 0.206
$d_c^{conv,h}$ (ft) (m)	0.600 – 0.183	0.619 – 0.189	0.619 – 0.189
$d_c^{conv,v}$ (ft) (m)	0.544 – 0.166	0.544 – 0.166	0.544 – 0.166
H_{rad} (ft) (m)	26.867 – 8.189	24.673 – 7.520	28.217 – 8.601
H_{conv} (ft) (m)	5.435 – 1.657	5.435 – 1.657	5.435 – 1.657
H_{total} (ft) (m)	82.302 – 20.086	80.108 – 24.417	113.652 – 34.641
W_{rad} (ft) (m)	18.275 – 5.570	16.503 – 5.030	19.653 – 5.990
W_{conv} (ft) (m)	5.208 – 1.587	5.349 – 1.630	6.586 – 2.007
Nt_{shield}	8	8	10
$Nt_{rad}^{sidewall}$	78	66	82
Nt_{rad}	104	88	110
Nt_{conv}	64	64	80
E_l (ft) (m)	39.543 – 12.053	29.543 – 9.005	39.543 –12.053
L_{oil} (ft) (m)	6,643.190 – 2024.844	4,490.506 – 1368.706	7,513.132 – 2,290.003
A_{rad} (ft^2) (m^2)	4,844.879 – 450.104	3,062.785 – 284.542	5,124.391 – 476.071
A_{conv} (ft^2) (m^2)	32,694.292 – 3,037.398	24,426.215 – 2,269.269	40,867.864 – 3,796.747
A_s (ft^2) (m^2)	64.427 – 5.985	52.288 – 4.858	83.541 – 7.761
A_b (ft^2) (m^2)	0.666 – 0.062	0.666 – 0.062	0.666 – 0.062
A_{of} (ft^2) (m^2)	12.253 – 1.138	12.253 – 1.138	12.253 – 1.138
A_{ot} (ft^2) (m^2)	12.919 – 1.200	12.919 – 1.200	12.919 – 1.200

We attempted to solve the design optimization problem using BARON and ANTIGONE, both global solvers, as well as DICOPT and SBB, which are local solvers. the addition of several binary variables and the corresponding equations to choose the discrete values of the independent design variables were needed for the mathematical programming model. These additional equations are presented in Supplemental Material S6.

To test the correctness of the equations implemented, we fixed the geometrical values and run without the initial values of the other dependent variables using BARON. The model run and found feasible solutions but it failed to satisfy the 2% tolerance gap after 2 h and found a solution featuring a 2.8% gap. This proved that the model is correct and suggested that mathematical programming is not a good tool for this design optimization. Without any initial value, BARON, ANTIGONE, DICOPT, and SBB are unable to find a feasible solution. ANTIGONE cannot find a feasible solution with initial values or fixing the independent geometry variables. When BARON is given the solution as initial values, it did not converge. We did the same experiments with the other solvers, but they all failed to converge.

Table 6 – Set Trimming Progression, Smart Enumeration Simulations and Computational time.

	Example 1	Example 2	Example 3
Initial number of candidates	9,000,000	9,000,000	9,000,000
STEP[1]: $\frac{H}{W} > \frac{H}{W\_Min}$	6,660,600	6,660,600	6,660,600
STEP[1]: $\frac{H}{W} < \frac{H}{W\_Max}$	3,619,800	3,619,800	3,619,800
STEP[2]: $\frac{L}{W} > \frac{L}{W\_Min}$	731,160	731,160	731,160
STEP[2]: $\frac{L}{W} < \frac{L}{W\_Max}$	663,900	663,900	663,900
STEP[3]: $\frac{L \times W \times H}{\pi \hat{D}_O E_f N t^{rad}} > BoxSize\_\min$	573,720	573,720	573,720
STEP[3]: $\frac{L \times W \times H}{\pi \hat{D}_O E_f N t^{rad}} < BoxSize\_\max$	297,000	297,000	297,000
STEP[4]: $d_c^{rad} \geq d_o + \hat{\varepsilon}_r$	297,000	297,000	297,000
STEP[5]: $d_c^{conv,h} \geq 2l_f + d_o$	254,760	254,760	254,760
STEP[6]: $\sqrt{(d_c^{conv,v})^2 + \left(\frac{d_c^{conv,h}}{2}\right)^2} \geq 2l_f + d_o$	254,760	254,760	254,760
STEP[7]: $D_s > W - 2W_l$	151,320	151,320	151,320
STEP[8]: $Vel_{oiltube} \leq 6$ [ft/sec]	151,320	151,320	128,580
STEP[9]: $\Delta P_{oiltube} \leq 5760$ [lb_f/ft^2] = (40 psi)	21,396	50,508	9,104
STEP[10]: $G_{LB} \leq G_{MAX}$ (=0.4 [lb/ft^2 sec])	21,396	50,508	9,104
STEP[11]: $G_{UB} \geq G_{MIN}$ (=0.3 [lb/ft^2 sec])	13,264	19,828	4,784
STEP[12]: $T_C < \hat{T}_{fb,Max} - \Delta\hat{T}_{\min}$	13,264	19,828	4,784
STEP[13]: $T_c > \hat{T}_i$	13,264	16,628	4,784
STEP[14]: $T_{fb} < \hat{T}_{fb,\max}$	13,264	16,628	4,784
STEP[15]: $T_{fb} > \hat{T}_{fb,\min}$	13,264	16,628	4,784
STEP[16]: $T_{fb}^{UB} < T_c^{LB}$	13,264	16,628	4,784
STEP[17]: $T_s > \hat{T}_i + \Delta\hat{T}_{\min}$	11,224	16,580	2,320
STEP[18]: $T_s < T_{fb} - \Delta\hat{T}_{\min}$	11,224	16,580	2,320
STEP[19]: $\min(Q_{Conv}^{UB1}, Q_{Conv}^{UB2}) < \max(Q_{Conv}^{LB1}, Q_{Conv}^{LB2})$	7,776	4,844	2,260
STEP[20]: $g(\rho_a - \hat{\rho}_{g,o})H \geq (1+\varepsilon)(\Delta\hat{P}_b + \sum F_{LB})$	7,776	4,844	2,260
Number of simulations in the Smart Enumeration step	449	258	222
Computational time (s)	77.8	152.5	211.1

9. Conclusions

In this work, we solved the design optimization problem of fired heaters using Set Trimming followed by Smart Enumeration. Set trimming uses the inequality constraints of the problem to reduce quickly and considerably the number of solution candidates by eliminating a large fraction of infeasible candidates, as illustrated in three different examples. Finally, the Smart Enumeration procedure allows the identification of the global optimum through the simulation of a small number of candidates, compared with the initial search space. The procedure stops when it is impossible to reduce the objective function, therefore it always identifies the global optimum. Because of the high nonlinearity of the problem, different local and global optimization solvers failed to converge.

Additionally, our procedure is robust, simple initial estimates (we use averages of the variables bounds) are only necessary to solve the fired heater model for different solution candidates during the Smart Enumeration. Solving the fired heater model for each candidate, is similar to a simulation problem (the geometry is fixed for each candidate and the fuel consumption is determined after setting the outlet oil temperature) and corresponds to the solution of a system of nonlinear equations. Our numerical experiments did not show convergence issues related to these candidates' simulations.

Nomenclature

The nomenclature is available in Supplemental Material S7.

Data Availability

The GAMS code is available upon request.

Declaration of Competing Interest

The authors declare that they have no known competing financial interests or personal relationships that could have appeared to influence the work reported in this paper.

Acknowledgements

André L. H. Costa thanks the National Council for Scientific and Technological Development (CNPq) for the research productivity fellowship (Processes 310390/2019–2). André L. H. Costa also thanks the financial support of Prociência Program (UERJ). Miguel J. Bagajewicz would like to thank the Universidade do Estado do Rio de Janeiro (Brazil) for its scholarship as Visiting Researcher - PAPD Program and the Universidade Federal do Rio de Janeiro (Brazil) for its support as visiting professor.

Appendix A. Supporting information

Supplementary data associated with this article can be found in the online version at doi:10.1016/j.cherd.2023.08.002.

References

Asker, M., Turgut, O.E., Coban, M.T., 2014. A review of non iterative friction factor correlations for the calculation of pressure drop in pipes. J. Sci. Techon. 4 (1), 1–8.

Cao, E., 2009. Heat transfer in process engineering. McGraw-Hill.

Costa, A., Bagajewicz, M., 2019. 110th anniversary: on the departure from heuristics and simplified models toward globally optimal design of process equipment. Ind. Eng. Chem. Res. 58, 18684–18702.

Couper, J.R., Penney, W.R., Fair, J.R., Walas, S.M., 2012. Chemical Process Equipment. Selection and Design, third ed. Elsevier, pp. 202–210.

Haratian, M., Amidpour, M., Hamidi, A., 2019. Modeling and optimization of process Fired heaters. Appl. Therm. Eng. 157, 1–12.

Ibrahim, H.A., Al-Qassim, M., 2013. Calculation of radiant section temperatures in fired process heaters. Chem. Eng. Sci. 1 (4), 55–61.

Ibrahim, H.A., Al-Qassimi, M., 2010. Simulation of heat transfer in the convection section of fired heaters. Per. Pol. Chem. Eng. 54 (1), 33–40.

Jegla, Z., Kilkovský, B., Turek, V., 2016. Novel approach to proper design of combustion and radiant chambers. Appl. Therm. Eng. 105, 876–886.

Jethva, M.N., Bhagchandani, C.G., 2013. Fired heater design and simulation. Int. J. Eng. Trends Tech. 4 (2), 159–164.

Jin, Z.L., Qiwu, D., Minshan, L., 2008. Heat exchanger network synthesis with detailed heat exchanger design. Chem. Eng. Technol. 31 (7), 1046–1050.

Karimi, M., Kargari, A., Behbahani-nia, S.A., Sanaeepur, H., 2019. Heat recovery and optimizing design of furnaces in the gasoline-kerosene units of Tabriz oil refining company. Appl. Therm. Eng. 161, 114–136.

Kazi, S.R., Short, M., Isafiade, A.J., Biegler, L.T., 2021. Heat exchanger network synthesis with detailed exchanger designs—2. Hybrid optimization strategy for synthesis of heat exchanger networks. AIChE J. 67, e17057.

Masoumi, M.E., Izakmehri, Z., 2011. Improving of refinery furnaces efficiency using mathematical modeling. Int. J. Model. Optim. 1 (1), 74–79.

Mizutani, F.T., Pessoa, F.L.P., Queiroz, E.M., Hauan, S., Grossmann, I.E., 2003. Mathematical programming model for heat-exchanger network synthesis including detailed heat-exchanger designs. 2. Network synthesis. Ind. Eng. Chem. Res. 42, 4019–4027.

Mussati, S., Manassaldi, J.I., Benz, S.J., Scenna, N.J., 2009. Mixed integer nonlinear programming model for the optimal design of fired heaters. Appl. Therm. Eng. 29 (11–12), 2194–2204.

Ponce-Ortega, J.M., Serna-Gonzáles, M., Jiménez-Gutiérrez, A., 2007. Heat exchanger network synthesis including detailed heat exchanger design using genetic algorithms. Ind. Eng. Chem. Res. 46, 8767–8780.

Ravagnani, M.A.S.S, Caballero, J.A., 2007. Optimal heat exchanger network synthesis with the detailed heat transfer equipment design. Comp. Chem. Eng. 31, 1432–1448.

Short, M., Isafiade, A.J., Fraser, D.M., Kravanja, Z., 2016. Synthesis of heat exchanger networks using mathematical programming and heuristics in a two-step optimisation procedure with detailed exchanger design. Chem. Eng. Sci. 144, 372–385.

Silva, A.P., Ravagnani, M.A.S.S., Biscaia Jr., E.C., 2008. Particle swarm optimisation in heat exchanger network synthesis including detailed equipment design. ESCAPE18 2008.

Varghese, J., Bandyopadhyay, S., 2012. Improved area-energy targeting for fired heater integrated heat exchanger networks. Chem. Eng. Res. Des. 90, 213–219.

Wimpress, N., 1978. Generalized method predicts fired-heater performance. C. F. Braun Co., May 22.

Xiao, W., Wang, K., Jiang, X., Li, X., Wu, X., Hao, Z., He, G., 2019. Simultaneous optimization strategies for heat exchanger network synthesis and detailed shell-and-tube heat-exchanger design involving phase changes using GA/SA. Energy 183, 1166–1177.